



# Vibration spectroscopic evidence for different interactive modes of iodide on gibbsite in humic acid mediation

L. Jayarathna<sup>1</sup> · M. Makehelwala<sup>2</sup> · A. Bandara<sup>3</sup> · R. Weerasooriya<sup>1</sup>

Received: 26 January 2018 / Revised: 24 May 2018 / Accepted: 25 May 2018  
© Springer-Verlag GmbH Germany, part of Springer Nature 2018

## Abstract

Determination of the fate of iodide and associated species is an important scientific question from environmental and nuclear energy perspectives. The chemical kinetics of iodide adsorption on gibbsite was examined in the presence of humic acids (HA). The iodide retention was highest in HA-coated gibbsite ( $\Gamma_1$  15.5  $\mu\text{mol m}^{-2}$ ; pH 6.50) and lowest in HA-iodide-gibbsite ternary systems ( $\Gamma_1$  9.56  $\mu\text{mol m}^{-2}$ ; pH 6.50). Both inter- and intralayer OH groups have distinguishable IR manifestations for iodide retention on gibbsite. In HA-coated gibbsite, the enhanced iodide retention was ascribed to direct bonding with surface Al-sites.

**Keywords** Iodide · Gibbsite · Humic acid · Adsorption · IR spectroscopy

## Introduction

Iodine is a biologically active element that occurs in the environment both from lithogenic ( $^{127}\text{I}$  or I hereafter) and anthropogenic ( $^{129}\text{I}$  and  $^{131}\text{I}$ ) sources. Lithogenic iodine, I, is nonradioactive, and is essential for human and animal health for their production of thyroid hormones, and also for the proper functioning of the thyroid gland. Iodine deficiency that can lead to severe metabolic disorders is a global public health issue [1]. However, both  $^{129}\text{I}$  and  $^{131}\text{I}$  are strongly radioactive and are these hazardous that often enter the environment from nuclear power plants [2, 3]. The  $^{129}\text{I}$  has a long half-life ( $t_{1/2} = 1.6 \times 10^6$  year) and possesses high mobility [4]. Irrespective of its source, iodine dominates in three oxidation states, viz. 0 (elemental I),  $-1$  ( $\Gamma^-$ ), and  $+5$  ( $\text{IO}_3^-$ ). In extremely oxygenated waters (Eh  $\sim +1000$  mV),  $\text{IO}_3^-$  may be present in significant proportions [5]. When the environment is extremely acidic (pH  $< 3$ ), molecular  $\text{I}_2$  is formed either from the reduction of

$\text{IO}_3^-$  or oxidation of  $\Gamma^-$ . Over the entire geochemical domain of natural waters, the iodide ion ( $\Gamma^-$ ) dominates, and it can therefore be used as a probe to assess different geochemical processes [6]. Iodide showed no hydrophobicity to most of minerals; hence, its interactions with geologic substrates are considered elemental or electrostatic in nature [7]. One of the essential factors controlling iodide mobility is the ability of soils, or associative surface-active substrates to retain or release it. The iodide concentrations in natural soils and waters are typically very low, i.e., sandy soils, 2.1 and 70  $\text{mg kg}^{-1}$  marine soils; hence, its bioavailability is controlled by adsorptive/desorptive mechanisms [8].

This work was aimed at determining the adsorption mechanism/s of iodide onto gibbsite in the presence of natural organic matter. Gibbsite and humic substances were chosen due to their ubiquity in nature. Hitherto date, the available literature depletes with respect to iodide adsorption on gibbsite or analog solids. Therefore, some comparisons were made with other minerals [9–14]. Iodide showed weak or no affinity for muscovite, calcite, quartz, montmorillonite, or kaolinite [15, 16]. However, illite, allophone, or imogolite showed high affinity for iodide by reversible physical adsorption to the pH dependent edge sites and not by irreversible fixation onto the clay structure [10]. Particularly for clay minerals, it is important to realize that iodide retention capacity as measured by partition coefficients did not follow trends of theoretical mineral unit charge or surface area values [11]. MacLean et al. (2004) [17] have shown that iodide/bacteria interactions are electrostatic that depends on pH, solid/

✉ L. Jayarathna  
lakmalipj@yahoo.co.uk

<sup>1</sup> Environmental Science Program, National Institute of Fundamental Studies, Kandy, Sri Lanka

<sup>2</sup> Research Center for Eco-Environmental Science, Chinese Academy of Science, Beijing, China

<sup>3</sup> Department of Chemistry, University of Peradeniya, Peradeniya, Sri Lanka

solution ratio, and ionic strength. The XANES data suggest that iodide adsorbs to hydrous ferrous oxides without undergoing changes in its hydration state [13]. Dai et al. [12] noted a strong correlation between iodide sorption capacity and natural organic matter content in soils without conclusive interpretations. These investigations emphasized the potential role played by natural organic matter in the retention of iodide by minerals. Further, the chemical data do not provide sufficient insight into the exact bonding nature between iodide and gibbsite [6, 9–11, 18]. In the present work, DRIFT infrared spectroscopy was used to probe gibbsite and iodide interactions in the presence of humic substances. The IR spectra of minerals (above the fundamental absorption frequency of the crystal) included a pattern characteristic for each mineral. In the region of high frequency (3500–4000  $\text{cm}^{-1}$ ), the observed absorption bands characterize the vibration of surface hydroxyls, which can be treated as local variations of the admixture atom (H) on the surface. It has also been established that spectroscopy can give direct data on the vibrations of cation-oxygen bonds on the surface, i.e., on spectral images of surface vibrations of an inherent nature [19].

## Materials and methods

**Materials** Gibbsite was received from ALCOA, Australia. The pertinent physicochemical properties of gibbsite and water interface are shown below [7]. All chemicals were from Fluka (Switzerland), Sigma (USA), or BDH (UK). De-mineralized, distilled water was used to prepare all reagents.

**Methods** All chemical kinetic experiments of iodide adsorption on gibbsite were conducted either in distilled water or  $\text{NaNO}_3$  at 298 K. The effect of humic acid (HA) on iodide adsorption by gibbsite was also examined. In one set of experiments, both HA and iodide ions were introduced simultaneously, i.e., *HA/I-gibbsite*. Chemical kinetics of iodide adsorption on gibbsite was determined as a function of pH, iodide, and solid content. Relevant experimental details are well documented [7]; hence, only a brief outline is given below.

Unless otherwise mentioned, for adsorption kinetics, a batch suspension was prepared with 5  $\text{g L}^{-1}$  of *gibbsite* or *HA-coated gibbsite*. The concentration of the background electrolyte was adjusted to 0.01 M with 5 M  $\text{NaNO}_3$ . The solid to solution ratio was kept at 1:100 (*w/w*) to promote high percentages of iodide uptake. The gibbsite samples were pre-equilibrated with  $\text{NaNO}_3$  for 12 h prior to spiking with iodide. In all experiments, the pH of the equilibrated suspension was monitored and adjusted to a desired value using a Ross Sure-Flow electrode (Orion Research, 81-03). In a typical kinetic experiment, the batch solution was spiked with known concentration of iodide in the range 1–10 mM, and sample aliquots were withdrawn at pre-defined time intervals.

The amount of iodide adsorbed was determined by analyzing the supernatant, following the solid-liquid separation by membrane filtration through 0.45  $\mu$ . An iodide ion selective electrode, (Orion Res., 94-53) was used for iodide activity determination. Recoveries of spiked analysis were always around 93–96%.

To determine the effect of HA on iodide adsorption by gibbsite, a separate series of experiments were carried out. A 1000  $\text{mg L}^{-1}$  stock of HA was prepared by dissolving 1 g HA (Sigma-Aldrich, USA) in 0.12 M NaOH. To ensure optimal dispersion, the HA mixture was stirred continuously for 12 h. Afterwards, the HA suspension was used in two ways: In one way, a series of 100  $\text{mg L}^{-1}$  HA and 5 mM iodide solutions were prepared and the pH was matched with the gibbsite suspension to a desired value. Afterwards, the gibbsite suspension was spiked with HA/I. The concentrations of iodide and HA were 5 mM and 100  $\text{mg L}^{-1}$  respectively. Alternatively, the HA-coated gibbsite was prepared according to following method. A mass of 2.5 g of gibbsite and 100  $\text{mg L}^{-1}$  stock solution of HA was mixed in 500 mL 0.01 M  $\text{NaNO}_3$  and equilibrated at a desired pH for 12 h. The HA-coated gibbsite was separated by centrifugation into a vessel containing 500 mL in 0.01 M  $\text{NaNO}_3$  at the same pH. The chemical kinetics of iodide adsorption on HA-coated gibbsite was carried out according to the procedures given earlier in this section. For Fourier transform infrared analyses, the solid part of the slurry after filtration was dried in an oven at 40  $^\circ\text{C}$ . Infrared spectra were obtained using a Nicolet 6700 FTIR at 4  $\text{cm}^{-1}$  resolution under DRIFT mode. Prior to spectral analysis, all samples were well mixed with KBr at 1:100 (*w/w*) ratios to a desired dilution.

## Results and discussion

Chemical kinetics of iodide adsorption on gibbsite at initial iodide concentration of 5 mM in 0.01 M  $\text{NaNO}_3$  and pH 6.50 is shown in Fig. 1. Similar plots were obtained for different concentrations of initial iodide, i.e., 5–10 mM and gibbsite, i.e., 5–50  $\text{g L}^{-1}$  (data not shown). In all cases, the experimental protocols of sample preparation were, *A. I-gibbsite*: gibbsite interacted with iodide, *B. HA-coated gibbsite*: gibbsite was coated with HA prior to its interaction with iodide, and *C. HA/I-gibbsite*: gibbsite was interacted with HA and iodide simultaneously. Irrespective of the mode of preparation, the kinetic plots shown in Fig. 1 can be divided into three broad regions designated as I, II, and III. The iodide adsorption on gibbsite is initially fast (region I), which has reached an optimum (region II) then decreases to a plateau (region III) indicating that the overall iodide sorption kinetics is complex.

As noted in region II, out of the three experimental protocols employed: HA-coated gibbsite showed an enhancement of iodide retention ( $K_d$  4.06 at pH 4.01), whereas it was

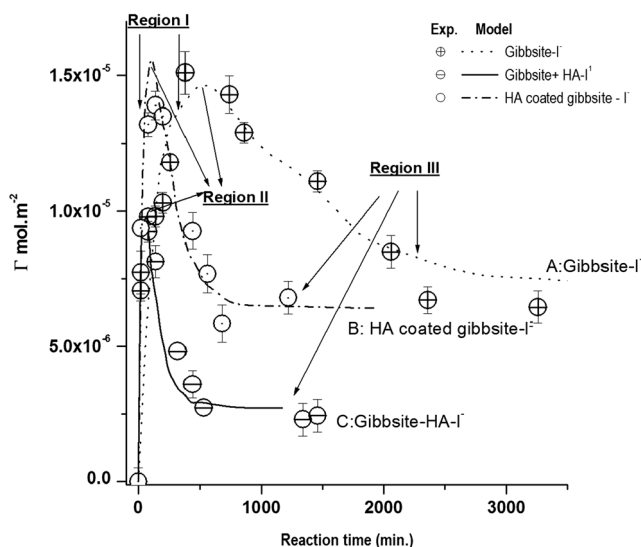


**Fig. 1** Iodide adsorption density in 0.01 M NaNO<sub>3</sub> as a function of reaction time. Symbols represent data; lines represent modeled data using reactions given in Table 1. pH ~ 6.50. Similar data were obtained at pH 4 and 6 (data not given). Initial iodide = 25 mM, pH 6.50 T = 298 K

minimal on HA/I-gibbsite ( $K_d$  0.37 at pH 4.00). Exact reasoning for this observation is not yet predicted. It appears that HA preferably interacts with gibbsite sites forming favorable conditions for subsequent adsorption of iodide. However, when HA and iodide coexist, HA competes with iodide for same gibbsite sites, which results in a reduction of iodide adsorption. The crystallographic site density of gibbsite is  $8.10 \mu\text{mol m}^{-2}$  [20]. Even at its optimal adsorption, iodide covers only a small fraction of the total sites ( $0.28 \mu\text{mol m}^{-2}$ ), which results a surface with largely unsaturated sites. The amount of surface sites, used in a given equilibrium is frequently much less than its total amount. For example, at the end of the first 5 min, after approaching the optimal conditions (region II), the iodide adsorbed was  $16 \mu\text{mol m}^{-2}$  on the HA-coated gibbsite,  $14 \mu\text{mol m}^{-2}$  on gibbsite, and  $9 \mu\text{mol m}^{-2}$  on HA/I-gibbsite, which accounted for 3.1, 2.6, and 2.5% of the total iodide adsorbed. The iodide adsorption density on gibbsite samples follows the order  $\Gamma_I^{\text{HA-coated}} \geq \Gamma_I^{\text{I-gib}} \geq \Gamma_I^{\text{gib}}$  within the first 40 min.

The kinetic data for iodide adsorption by gibbsite can be interpreted considering two site types: reversible site type designated as  $\equiv\text{AlO}_R\text{H}$ , where iodide adsorption occurred rapidly, and quasi- or irreversible sites designated as  $\equiv\text{AlO}_I\text{H}$ , where iodide adsorption is comparatively slow. The irreversibility of iodide adsorption on gibbsite believes to involve a complex reaction series. When iodide and gibbsite are interacted, the initial adsorption believed to occur rapidly onto  $\equiv\text{AlO}_R\text{H}$  (region I). As time evolved, the iodide adsorption onto  $\equiv\text{AlO}_I\text{H}$  sites also becomes appreciable. Both of these processes deplete iodide activity in solution offsetting equilibrium, which was restored releasing surface bound iodide preferably from  $\equiv\text{AlO}_R\text{H}$  sites. As shown in Fig. 1, this results in a depression

in time evolved iodide adsorption curves. Afterwards, iodide adsorption density maintains an almost a constant value, which implies comparatively strong affinity sites, i.e.,  $\equiv\text{AlO}_I\text{H}$  for iodide adsorption.

The initial rate of iodide adsorption was calculated from the data shown in the region I (Fig. 1). At a given pH, the initial kinetics of iodide adsorption on gibbsite is pseudo first order with respect to both iodide and surface site concentration and the initial rate constants are given in Table 1. The initial rate constants are empirical; they do not directly correspond to any elementary reaction steps implicitly; however, they do reflect a composite effect of several reactions. The exact identification of each of these microscopic steps involved is not possible with the data shown. Nevertheless, a partial understanding of the adsorption mechanism is possible from these data via kinetic modeling. The time dependent  $\Gamma_I$  data were modeled with a nonlinear optimization algorithm according to the simple kinetic model given in Table 1. The optimized rate constants are also shown in the same table. In all cases, e.g., gibbsite/iodide, HA-coated gibbsite/iodide, and HA/I-gibbsite, this model seems to be valid. This implies that the iodide adsorption on gibbsite always occurred through  $\equiv\text{AlO}_R\text{H}$  and  $\equiv\text{AlO}_I\text{H}$  sites irrespective of the sample treatment methods of gibbsite. These conclusions are reinforced by spectroscopic data as discussed below.

## IR spectroscopy

In order to probe the spectral evidence for iodide and gibbsite/HA-coated gibbsite interactions, IR data were collected in 400–4000  $\text{cm}^{-1}$  range, and the results obtained are shown in Fig. 1a–d and support documents.

## IR spectrum of HA

As shown in Fig. 2, the IR spectrum of HA is featureless in the wavelength range 400–4000  $\text{cm}^{-1}$ . The stacking of HA molecules themselves favor H-bonding without leaving any OH moieties to the interface as such the spectrum will not exhibit any bands due to isolated OH groups. However, the broad band around 1630  $\text{cm}^{-1}$  is due to H-O-H bending resulting from strong H-bonding (positions not shown in figure). The bands due to C-H 1, 4 substitutions appear at 798, 822, and 837  $\text{cm}^{-1}$  in HA. Bands at 2852, 2919, and 2964  $\text{cm}^{-1}$  are ascribed to methyl C-H stretching in HA. A broad band appears at 3440  $\text{cm}^{-1}$  in HA for H bonded OH stretching and small bands at 3695, 3756, and 3841  $\text{cm}^{-1}$  in HA are due to primary, secondary, and tertiary OH stretching respectively.

In HA-coated gibbsite, the IR spectrum showed distinct features. A broad band at 756  $\text{cm}^{-1}$  indicates HA and gibbsite interactions; the bands at 802 and 827  $\text{cm}^{-1}$  appeared due to band-overlapping. The bands over 3670  $\text{cm}^{-1}$  disappeared

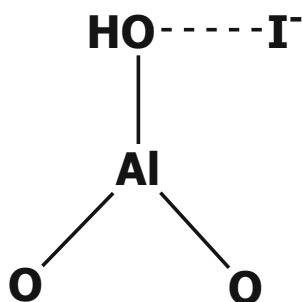
**Table 1** Proposed reaction stoichiometries of iodide adsorption by gibbsite used in kinetic modeling

Chemical kinetic modeling data Parameter/reaction	Rate constant, min <sup>-1</sup>		
	Gibbsite	Gibbsite HA + I <sup>-</sup>	HA-coated gibbsite I <sup>-</sup>
$2 \equiv \text{Al}_i\text{OH} + \text{I}^- \rightarrow 2[\equiv \text{Al}_i\text{OH}\cdot\text{I}]$	6.4E-9	1.1E-8	2.1E-8
$\equiv \text{Al}_R\text{OH} + \text{I}^- \rightarrow \equiv \text{Al}_R\text{OH}\cdot\text{I}^-$	1.5E-5	8.5E-5	5.5E-5
$\equiv \text{Al}_R\text{OH}\cdot\text{I}^- \rightarrow \equiv \text{Al}_R\text{OH} + \text{I}^-$	5.0E-3	5.0E-2	2.0E-2
Initial rate method data			
$d[I]_{\text{initial}}/dt = k[\text{gibbsite}]_i^m [I]_i^n$			
Different iodide loading			
$d[I]_{\text{initial}}/dt = k' [I]_i^n$			
Rate constant (m mol L <sup>-1</sup> /min)	3.42E-2	4.19E-2	4.36E-2
Different gibbsite loading			
$d[I]_{\text{initial}}/dt = k'' [\text{gibbsite}]_i^m$			
Rate constant (m mol L <sup>-1</sup> /min)	-4.25E0	2.48E0	5.87E-1
Partition coefficients, $K_d$ (pH)			
	4.699 (3.20)	0.368 (3.20)	4.060 (4.91)
	0.676 (5.35)	0.308 (5.30)	0.170 (7.20)
	0.419 (8.50)	0.243 (8.50)	0.130 (8.12)

The iodide gibbsite complex shown under Scheme 1 was used to model reaction (1), whereas reaction (2) was used to model the surface complexes under Scheme 2. The surface Scheme 3 was not taken into account

with the shift in some other bands when compared to the spectrum of bare gibbsite. These changes can be ascribed to HA interactions with gibbsite occurring via H-bonding and also probably due to some chelating with aluminum ions on gibbsite. Bands that appear at 633, 642, and 663 cm<sup>-1</sup> are for -C≡H bending in humic acid. The bands at 702, 725, and 752 cm<sup>-1</sup> are due to mono-substitution of aromatic rings in HA. In the HA/gibbsite sample, the broad band at 756 cm<sup>-1</sup> indicates interactions between HA and gibbsite. Further in the HA/gibbsite spectrum, the band at 642 cm<sup>-1</sup> disappears completely and the band at 633 cm<sup>-1</sup> is shifted to 636 cm<sup>-1</sup>. In the presence of iodide in the system, there is no major change in the spectrum; however, the bands at 636 and 756 cm<sup>-1</sup> shift to a lower frequency region 629 and 752 cm<sup>-1</sup>, respectively.

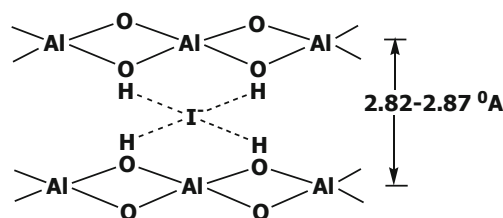
Investigations of the IR spectra of oxides in 3000–4000 cm<sup>-1</sup> region above fundamental frequencies can yield direct information on surface hydroxyl groups and their



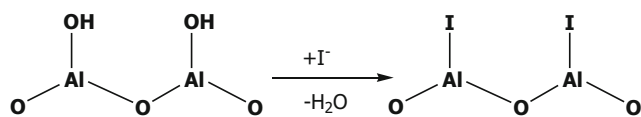
Scheme 1

nonhomogeneity. A reason for the appearance of several bands due to free hydroxyl groups is the capability of identifies the oxygen atom of OH groups in different chemical nature. Hence, their number should exert a decisive influence on the vibration frequency [19]. The DRIFT spectra of gibbsite showed fine resolutions between 3465 and 3397 cm<sup>-1</sup> when compared to their transmission spectral counterparts [21]. Due to enhanced sensitivity, all subsequent spectra were taken under DRIFT mode. The wave number region of the characteristic OH stretching vibrations (3000–4000 cm<sup>-1</sup>) is shown in Figs. 3 and 4 for I-gibbsite, HA-coated gibbsite, and HA/I-gibbsite.

In agreement with previous data [21, 22], for gibbsite spectral trace of OH stretching region is totally resolved into seven bands, viz. 3293, 3378, 3396, 3430, 3465, 3525, and 3118 cm<sup>-1</sup> (support documents, Fig. 1a). The bands at 3618, 3525, and 3465 cm<sup>-1</sup> are linked with OH stretching modes. The bands at 3465, 3378, and 3396 cm<sup>-1</sup> are related with H-bonds between layers, and the bands at 3618 and 3525 cm<sup>-1</sup> correspond to long H-bonds within the same plane. The OH-OH in plane separations larger than 3.36 nm probably involve



Scheme 2



Scheme 3

no interactions, hence occur in isolation [23, 24]. After interacting gibbsite with iodide, the  $3293\text{ cm}^{-1}$  band shifts to  $3310\text{ cm}^{-1}$ ; a new band appears at  $3213\text{ cm}^{-1}$  and the band at  $3465\text{ cm}^{-1}$  is broadened (Fig. 3a). As shown below, these observations clearly indicate interactions of gibbsite and iodide affecting OH stretching modes. Further, the corresponding surface sites are treated reversible, e.g.,  $\equiv\text{AlO}_R\text{H}$ . Additionally, four new bands at  $3670$ ,  $3708$ ,  $3730$ , and  $3749\text{ cm}^{-1}$  appear which are assigned to isolated hydroxyls that are free upon iodide loading. The ionic radii of iodide and interlayer distance of the gibbsite are comparable. As shown below, the iodide can be bound to interlayer hydroxyl sites via H-bonding. Due to the size of iodide, its movement to interlayer region is a slow process, and these sites are treated as irreversible, e.g.,  $\equiv\text{AlO}_I\text{H}$ .

The HA is a cross-link polymeric moiety, which has sites for H-bonding. The hydrophobic nature of HA repels it from aqueous phase to interface, which facilitate H-bonding. The disappearance of IR bands (i.e.,  $3670$ ,  $3708$ ,  $3730$ , and  $3749\text{ cm}^{-1}$ ), shifts of others ( $3293$  to  $3282\text{ cm}^{-1}$ ), and splitting of yet others ( $3465$  into  $3459$  and  $3479\text{ cm}^{-1}$ ) reflect intense H-bond formation with HA and the presence of free  $\equiv\text{AlO}_I\text{H}$  sites. The bands in the  $3670$ – $3750\text{ cm}^{-1}$  region disappear completely (Fig. 3b). This implies that the H-bonding is not perturbed upon HA addition. As shown in Fig. 4a when gibbsite is interacted with HA and iodide simultaneously

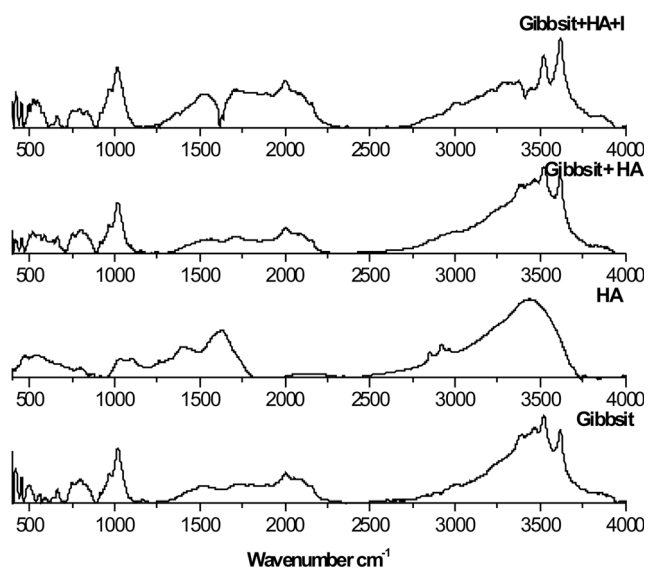


Fig. 2 Diffuse reflectance IR spectra in  $400$ – $4000\text{ cm}^{-1}$  of gibbsite, humic acid, humic acid-coated gibbsite, and gibbsite, humic acid, iodide system

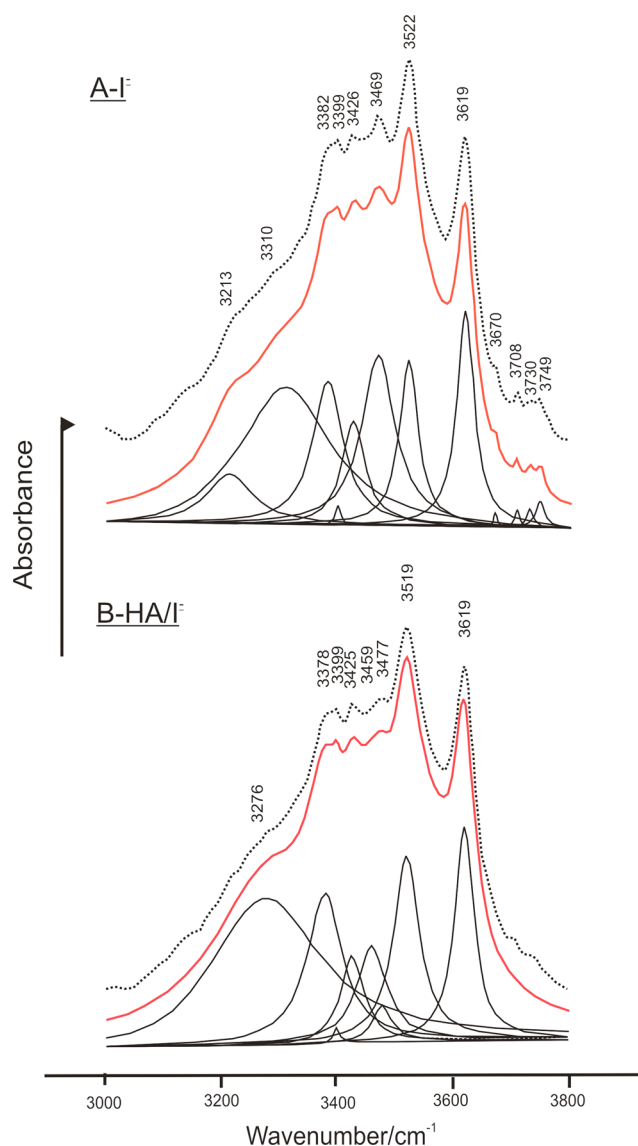
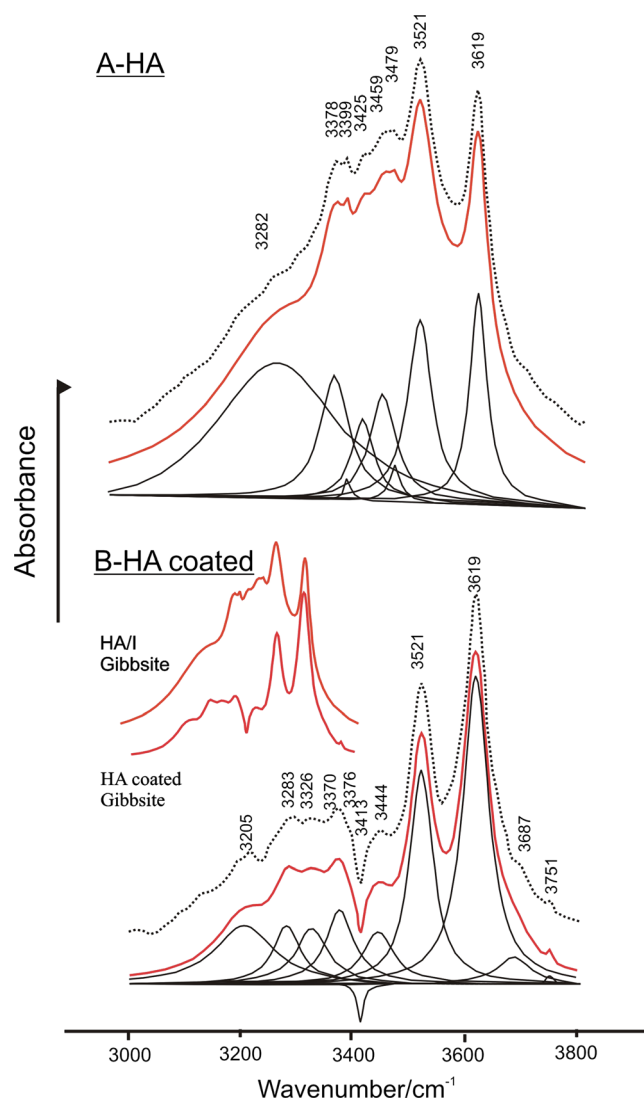


Fig. 3 Diffuse reflectance IR spectra in  $3000$ – $4000\text{ cm}^{-1}$  range. **a** Gibbsite adsorbed by  $\text{I}^-$ ; **b** gibbsite adsorbed by humic acid

(i.e., HA/I-gibbsite), the band splitting at  $3465\text{ cm}^{-1}$  disappears completely. Bands corresponding to isolated hydroxyls appear weak and the band at  $3293\text{ cm}^{-1}$  shifts to  $3282\text{ cm}^{-1}$ . Apart from these differences, the spectral traces of I-gibbsite and HA/I-gibbsite look alike exhibiting similar bonding as in Scheme 1 when HA-coated gibbsite is reacted with iodide (Fig. 4b); however, several significant spectral changes were observed. The band at  $3465\text{ cm}^{-1}$  has shifted to  $3444\text{ cm}^{-1}$ . A negative intensity appeared at  $3413\text{ cm}^{-1}$ . This is ascribed to conversion of  $\text{OH} \rightarrow \text{H}_2\text{O}$  by iodide as shown below (Scheme 3). The bands corresponds to the  $\text{OH}^-$  ( $3413\text{ cm}^{-1}$ ) is completely disappeared forming  $\text{H}_2\text{O}$  resulting of a sharp apparent reversal of negative intensity. Iodide ion seems interact with the vacant site. This results as an apparent reversal of relative intensity often misinterpreted as negative peak. To facilitate this dehydroxylation step, the presence of



**Fig. 4** Diffuse reflectance IR spectra in 3000–4000  $\text{cm}^{-1}$  range. **a** HA/I-gibbsite; **b** HA-coated gibbsite

solid bound HA and iodide ions is essential. The FTIR data were fitted for better peak resolving. The fitting requires inclusion of a peak at  $3413 \text{ cm}^{-1}$  with negative intensity because

**Table 2** Characterization of gibbsite

Parameter	Value
Specific surface area ( $\text{m}^2 \text{ g}^{-1}$ )	13
Average particle size ( $\mu\text{m}$ )	10
Site density	8.1

When pH is ranged between 4 and 8, the dominant anion species is free iodide, whereas according to 2-pK approach, the gibbsite surface is hydroxylated as  $\equiv\text{AlOH}$ ,  $\equiv\text{AlOH}_2^+$ , and  $\equiv\text{AlO}^-$ . Any solid surface is not smooth at an atomic scale. There exist kinks, steps, and terraces. The kink sites are surrounded by the smallest number of neighbors and have the highest surface energy. In gibbsite, these sites are believed to be unsaturated with  $\text{Al}^{3+}$ . Hence, the iodide adsorption should occur by these surface sites of different affinities

of negative peak in the data that cannot be accepted with the nature of data we have. Further, the intensity of the band at  $3619 \text{ cm}^{-1}$  increases significantly. These features are prominent in the spectral traces of iodide adsorption on HA-coated gibbsite Table 2.

## Conclusions

Chemical kinetics of iodide adsorption on gibbsite samples treated differently was modeled assuming two surface site types:  $\equiv\text{AlO}_R\text{H}$  and  $\equiv\text{AlO}_I\text{H}$ . In HA-coated gibbsite, the iodide retention has enhanced to some extent. The iodide retention was highest in HA-coated gibbsite and lowest in HA-iodide-gibbsite ternary systems. Both inter- and intralayer OH groups have distinguishable IR manifestations for iodide retention on gibbsite. Iodide formed surface complexes via H-bonding with terminal or interlayer surface OH groups. In HA-coated gibbsite, the enhanced iodide retention by direct bonding with surface Al-sites.

**Funding** This study was funded by the National Institute of Fundamental Studies, Hanthana road, Kandy and National research council grant number 16/015.

## Compliance with ethical standards

**Conflict of interest** All the authors declare that they have no conflict of interest.

## References

- Delange F, de Benoist B, Pretell E, Dunn JT (2001) Iodine deficiency in the world: where do we stand at the turn of the century? *Thyroid* 11(5):437–447
- Mann FM (2000) Hanford Immobilized Low Activity Waste (ILAW) Performance Assessment 2001 Version [Formerly DOE/RL-97-69] [SEC 1 & 2], CHG (US). *p*. Medium: ED; Size: 600 pages
- Xu C, Kaplan DI, Zhang S, Athon M, Ho YF, Li HP, Yeager CM, Schwehr KA, Grandbois R, Wellman D, Santschi PH (2015) Radioiodine sorption/desorption and speciation transformation by subsurface sediments from the Hanford Site. *J Environ Radioact* 139:43–55
- Um W, Serne RJ, Krupka KM (2004) Linearity and reversibility of iodide adsorption on sediments from Hanford, Washington under water saturated conditions. *Water Res* 38(8):2009–2016
- Michałowska-Kaczmarczyk AM, Toporek M, Michałowski T (2015) Speciation diagrams in dynamic iodide + dichromate system. *Electrochim Acta* 155:217–227
- Shetya WH, Young SD, Watts MJ, Ander EL, Bailey EH (2012) Iodine dynamics in soils. *Geochim Cosmochim Acta* 77(Supplement C):457–473
- Weerasooriya R, Dharmasena B, Aluthpatabendi D (2000) Copper-gibbsite interactions: an application of 1-pK surface complexation model. *Colloids Surf A Physicochem Eng Asp* 170(1):65–77

8. Seiler HG, Sigel H, Sigel A (1988) Handbook on toxicity of inorganic compounds. Marcel Dekker, New York. Medium: X; Size: Pages: 1069
9. Sazarashi M et al (1994) Adsorption of  $\Gamma^-$  ions on minerals for 129I waste management. *J Nucl Sci Technol* 31(6):620–622
10. Kaplan DI, Serne RJ, Parker KE, Kutnyakov IV (2000) Iodide sorption to subsurface sediments and illitic minerals. *Environ Sci Technol* 34(3):399–405
11. Kaufhold S, Pohlmann-Lortz M, Dohrmann R, Nüesch R (2007) About the possible upgrade of bentonite with respect to iodide retention capacity. *Appl Clay Sci* 35(1):39–46
12. Dai JL, Zhang M, Hu QH, Huang YZ, Wang RQ, Zhu YG (2009) Adsorption and desorption of iodine by various Chinese soils: II. Iodide and iodate. *Geoderma* 153(1):130–135
13. Nagata T, Fukushi K, Takahashi Y (2009) Prediction of iodide adsorption on oxides by surface complexation modeling with spectroscopic confirmation. *J Colloid Interface Sci* 332(2):309–316
14. Theiss FL, Couperthwaite SJ, Ayoko GA, Frost RL (2014) A review of the removal of anions and oxyanions of the halogen elements from aqueous solution by layered double hydroxides. *J Colloid Interface Sci* 417:356–368
15. Bors J, Dultz S, Riebe B (1999) Retention of radionuclides by organophilic bentonite. *Eng Geol* 54(1):195–206
16. Riebe B, Dultz S, Bunnenberg C (2005) Temperature effects on iodine adsorption on organo-clay minerals: I. Influence of pretreatment and adsorption temperature. *Appl Clay Sci* 28(1):9–16
17. MacLean LCW, Martinez RE, Fowle DA (2004) Experimental studies of bacteria-iodide adsorption interactions. *Chem Geol* 212(3):229–238
18. Ticknor KV, Cho Y-H (1990) Interaction of iodide and iodate with granitic fracture-filling minerals. *J Radioanal Nucl Chem* 140(1):75–90
19. Knözinger H, Davydov AA (1991) Infrared Spectroscopy of Adsorbed Species on the Surface of Transition Metal Oxides. J. Wiley & Sons; ISBN 0-471-91 813-X, Chichester, New York, Brisbane, Toronto, Singapore, 1990. 243 Seiten. *Berichte der Bunsengesellschaft für physikalische Chemie*. 95(4):543–543
20. Hiemstra T, Van Riemsdijk WH (1991) Physical chemical interpretation of primary charging behaviour of metal (hydr) oxides. *Colloids and Surfaces* 59:7–25
21. Weerasooriya R, Tobschall HJ, Wijesekara HKDK, Arachchige EKIAUK, Pathirathne KAS (2003) On the mechanistic modeling of As(III) adsorption on gibbsite. *Chemosphere* 51(9):1001–1013
22. Weerasooriya R, Tobschall HJ, Wijesekara HKDK, Bandara A (2004) Macroscopic and vibration spectroscopic evidence for specific bonding of arsenate on gibbsite. *Chemosphere* 55(9):1259–1270
23. Russell JD et al (1974) Surface structures of gibbsite goethite and phosphated goethite. *Nature* 248:220–221
24. Wang S-L, Johnston Cliff T (2000) Assignment of the structural OH stretching bands of gibbsite. *Am Mineral*:739